Published for SISSA by Springer

Received: *February 24, 2021*
Revised: *March 17, 2021*
Accepted: *April 1, 2021*
Published: *May 5, 2021*

Search for sub-millicharged particles at J-PARC

Jeong Hwa Kim, In Sung Hwang and Jae Hyeok Yoo[1]

Korea University,
145 Anam-ro, Seongbuk-gu, Seoul, 02841, Korea

E-mail: jailbraker@korea.ac.kr, his5624@korea.ac.kr, jaehyeokyoo@korea.ac.kr

Abstract: We studied the feasibility of an experiment searching for sub-millicharged particles (χs) using 30 GeV proton fixed-target collisions at J-PARC. The detector is composed of two layers of stacked scintillator bars and PMTs and is proposed to be installed 280 m from the target. The main background is a random coincidence between two layers due to dark counts in PMTs, which can be reduced to a negligible level using the timing of the proton beam. With $N_{\mathrm{POT}} = 10^{22}$ which corresponds to running the experiment for three years, the experiment provides sensitivity to χs with the charge down to 5×10^{-5} in $m_\chi < 0.2$ GeV/c^2 and 8×10^{-4} in $m_\chi < 1.6$ GeV/c^2. This is the regime largely uncovered by previous experiments. We also explored a few detector designs to achieve optimal sensitivity to χs. The photoelectron yield is the main driver, but the sensitivity does not have a strong dependence on detector configuration in the sub-millicharge regime.

Keywords: Fixed target experiments, Dark matter

ArXiv ePrint: 2102.11493

[1]Corresponding author.

https://doi.org/10.1007/JHEP05(2021)031

JHEP05(2021)031

Contents

JHEP05(2021)031

1 Introduction

Electric charge quantization is a long-standing question in particle physics. While Grand Unified Theories (GUTs) have typically been thought to preclude the possibility for particles that do not have integer multiple electron charge (millicharged particles hereafter), well-motivated dark-sector models [1, 2] have been proposed that predict the existence of millicharged particles while preserving the possibility for unification. Such models can contain a rich internal structure, providing candidate particles for dark matter. Recent results from the EDGES experiment [3] suggest that the observed 21-cm absorption profile can be explained if a fraction of dark matter is composed of millicharged particles [4].

One well-motivated mechanism that leads to millicharged particles is introducing a new U(1) in the dark sector with a massless dark-photon and a massive dark-fermion (χ) [5, 6]. In this scenario, the dark-photon and the photon in the Standard Model kinematically mix, and the charge of χ is determined by the size of the mixing. Therefore, depending on the strength of the mixing, χ can have an electric charge that is not an integer multiple. Hereafter, χ is used to denote millicharged particles.

A number of experiments have searched for millicharged particles, including an electron fixed-target experiment [7], proton-proton colliders [8–10], a proton fixed-target experiment [11] and neutrino experiments [12, 13]. A comprehensive review is in Reference [14]. In the parameter space of the charge (Q) and mass (m_χ), the region of $m_\chi > 0.1$ GeV/c^2 and $Q < 10^{-3}e$ is largely unexplored.

Proton fixed-target experiments provide a solid testing ground for χs. The particle flux is much larger than in collider experiments, and they can reach higher energy than electron fixed-target experiments. The sensitivity of such experiments to χs can reach beyond $Q \sim 10^{-3}e$ for a wide mass range from a few MeV/c^2 to a few GeV/c^2. This letter proposes a new experiment, SUBMET (SUB-Millicharge ExperimenT), which utilizes the 30 GeV proton beam at the Japan Proton Accelerator Research Complex (J-PARC) to search for χs in this unexplored region.

2 Production of millicharged particles at J-PARC

At proton fixed-target collisions at J-PARC, χs with charge Q can be produced from the decay of $\pi^0, \eta, \rho, \omega, \phi$ and J/ψ neutral mesons. The Υ production is not relevant because the center-of-mass energy is 7.5 GeV for the collisions between the 30 GeV proton beam and the fixed target. The lighter mesons ($\mathfrak{m} = \pi^0, \eta$) decay through photons ($\mathfrak{m} \to \gamma\chi\bar{\chi}$), while ρ, ω, ϕ, and J/ψ decay to a pair of χs directly ($\mathfrak{m} \to \chi\bar{\chi}$). In both cases, m_χ up to $m_\mathfrak{m}/2$ is kinematically allowed. The number of produced χs (N_χ) can be calculated by the equation in [15],

$$N_\chi \propto c_\mathfrak{m} \epsilon^2 N_{\rm POT} \times f\left(\frac{m_\chi^2}{m_\mathfrak{m}^2}\right) \tag{2.1}$$

where $c_\mathfrak{m}$ is the number of mesons produced per proton-on-target (POT), $N_{\rm POT}$ is the total number of POT, $\epsilon = Q/e$, and f is a phase space related integral. The $c_\mathfrak{m}$ of each meson is extracted using `PYTHIA8` [16], and the estimated values are $c_{\pi^0} = 1.9$, $c_\eta = 0.21$, $c_\rho = 0.24$, $c_\omega = 0.24$, $c_\phi = 4.9 \times 10^{-3}$, and $c_{J/\psi} = 2.5 \times 10^{-9}$. The result of the simulation is validated by comparing it with existing measurements. Particularly, the flux of muons passing through the beam dump [17] and the production rate of J/ψ [18] in the simulation and measurements are found to be in good agreement. Assuming $N_{\rm POT} = 10^{22}$ that corresponds to running the experiment for 3 years [19], the expected number of χs that reach the detector is in the order of 10^{16} at $\epsilon = 1$ and 10^8 at $\epsilon = 10^{-4}$.

3 Experimental site and detector concept

In J-PARC, a 30 GeV proton beam is incident on a graphite target to produce hadrons that subsequently decay to a pair of muon and muon neutrino in the decay volume. The remaining hadrons are then dumped in the beam dump facility. Since they are Minimum Ionizing Particles, muons can penetrate the beam dump and be identified by the muon monitor located behind the beam dump facility. The on-axis near detector, Interactive Neutrino GRID (INGRID) [20], is inside the Neutrino Monitor (NM) building located 280 m from the target. The space between the muon monitor and INGRID is filled with sand. The experimental site is illustrated in figure 1. The proton beam has a repetition rate of 1.16 s and each spill contains 8 bunches, which are separated by 600 ns [21]. The beam timing is available at the site, and this allows for a substantial reduction of backgrounds by $O(10^{-6})$.

If χs are produced, they penetrate the space between the target and the detector without significant energy loss because of their feeble interaction with matter. Therefore, they can be detected at the NM building if a detector sensitive to identifying such particles is installed. The area behind the V-INGRID on B2 ($\sim$ 30 m underground) is unoccupied and can be a potential detector site. The distance from the axis of the neutrino beam is ~ 5 m.

The detector concept proposed for this experiment is based on a similar proposal made in [22], sharing the idea to use a segmented detector with large scintillator bars. To be sensitive to charges below $10^{-3}e$, a thick sensitive volume is needed. It is advantageous to segment the large volume because it helps reducing backgrounds due to dark currents and shower particles from cosmogenic muons to a negligible level. It also allows for utilizing the

JHEP05(2021)031

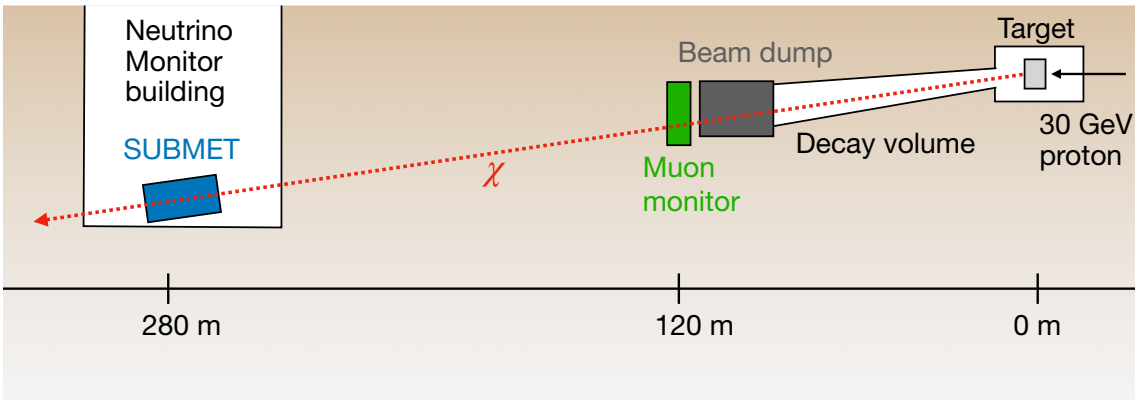

Figure 1. Illustration of the experimental site. χs are produced near the target and reach SUBMET after penetrating the beam dump, the muon monitor, and the sand. The detector is located 280 m from the target and approximately 30 m underground.

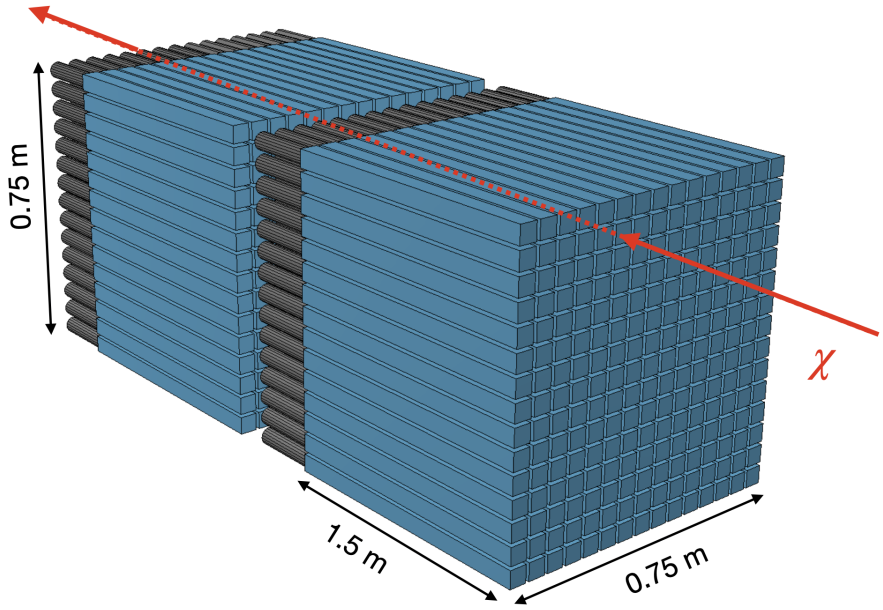

Figure 2. Demonstration of the SUBMET detector. There are two layers of stacked scintillator bars (blue). At one end of each bar, a PMT (black) is attached. χs penetrate both layers in a narrow time window.

directionality of the incident χs to further suppress non-pointing particles. The detector, as shown in figure 2, is composed of 2 layers of stacked $5 \times 5 \times 150$ cm^3 BC-408 plastic scintillator bars [26]. They are aligned such that the produced χs pass through both layers in a narrow time window. In each layer, there are 15×15 scintillator bars, so the area of the detector face is about 0.5 m^2. A prototype of a detector with a similar design has been installed at the LHC, and has shown robustness and sensitivity to χs [10].

JHEP05(2021)031

A photodetector is attached to the end of each scintillator bar to convert the photons to an electronic signal. Photomultipliers (PMTs) are suitable for this experiment because of their large area coverage, low cost, and low dark current. The total volume of the detector is approximately $0.75 \times 0.75 \times 3.5$ m^3 including the PMTs.

The signal acceptance rate, the fraction of χs that go into the detector area of 0.5 m^2 at 280 m from the target, is calculated as a function of distance from the beam axis to the detector. It is in the order of $O(10^{-4})$ and does not strongly depend on position, up to a few meters from the axis, since the detector is located far from the target. At 5 m the rate is only $\sim 10\%$ lower than the on-axis region. This provides some flexibility in selecting the location of the detector. The effect of energy loss and multiple Coulomb scattering in the sand is estimated to be negligible for the charge range of interest, particularly below $10^{-3}e$, so they have a small impact on the sensitivity of the experiment.

4 Background sources

χs that reach the detector will go through both layers within a $\sim$ 10 ns time window producing a coincidence signal. In this section, the background sources that can mimic this coincidence signal are discussed. They can be divided into three categories; random coincidence, beam-induced, and cosmic-induced backgrounds.

In PMTs, spurious current pulses can be produced by thermal electrons liberated from the photocathode. Therefore, a random coincidence of such pulses in different layers can be identified as a millicharge signal. The typical size of the pulses is very small, and this makes random coincidence the major background source in the $Q < 10^{-3}e$ regime. The rate of random coincidence can be large depending on the rate of the spurious pulses (dark count rate, DCR), even if the time window for the coincidence signal is 10 ns. The random coincidence rate is $nN^n\tau^{n-1}$, where n is the number of layers, N is the DCR, and τ is the coincidence time window. Using a typical PMT DCR of 500 Hz at room temperature, $n = 2$, and $\tau = 10$ ns, the random coincidence rate of two bars is 0.15 per year. There can be $15 \times 15 = 225$ such coincidence signals, so the total coincidence rate is $\sim$ 35 per year. The liberation of electrons is a thermal activity, which can be reduced by cooling the cathodes. With $N = 100$ Hz, the random coincidence background is reduced to 1.5 events per year.

Muons are produced from pion decays in the decay volume together with neutrinos. The density of quartz, which typically takes up the largest fraction of sand, is 2.65 g/cm^3 and $dE/dx = 1.699$ MeVcm^2/g [23], so the energy loss of a MIP in $>$ 100 m of sand is much larger than 30 GeV. Therefore, such beam-induced muons can not reach the detector. Although the muons from pion decays can not reach the detector, neutrinos can and may interact with the scintillator material to produce small signals. The number of neutrino interaction events in INGRID is $\sim 1.5 \times 10^8$ for $N_{\mathrm{POT}} = 10^{22}$ [24]. Since a large fraction of INGRID material is iron, the rate of neutrino interaction in INGRID can be used as an upper bound for SUBMET. One layer of SUBMET is approximately 30 times smaller, so the rate is $\sim 5 \times 10^6$ for $N_{\mathrm{POT}} = 10^{22}$ in one layer of SUBMET. Requiring coincidence in two layers, the expected number of events from this background source becomes negligible.

JHEP05(2021)031

The interaction of the neutrinos and the material of the wall of the NM building in front of the detector can produce muons that go through the detector. These muons can be identified and rejected by installing scintillator plates between the wall and the detector or by using the very large scintillation yield of a muon that can be separated from the millicharge signal.

Cosmic muons that penetrate the cavern or the materials above the detector can produce a shower of particles that is large enough to hit both layers simultaneously. In such events, the hits in multiple layers can be within the coincidence time window and will look like a signal event. The particles in the shower generate more photons than χs, so the signals from cosmic muon showers can be rejected by vetoing large pulses. As done to tag the muons produced in the wall of the NM building in front of the detector, scintillator plates can be installed covering the whole detector to tag any ordinary-charged particles or photons incident from the top and sides of the detector. These auxiliary components were proven to be effective in rejecting events with such particles [10]. In addition, the cosmic shower penetrates the detector sideways, leaving hits in multiple bars in the same layer, while χs will cause a smaller number of hits. A cosmic shower and signals from radioactive decays overlapping with dark current can be another source of background. Since the rate of this background depends on the environment strongly, a precise measurement can be performed *in situ* only.

To estimate the sensitivity of the experiment, we assume that the total background ($N_{\rm bkg}$) over three years of running is 5 events.

5 Sensitivity

The probability of detecting a χ in a detector with n layers is given by Poisson distribution $P = (1 - e^{-N_{\rm PE}})^n$, where $N_{\rm PE}$ is the number of photoelectrons. $N_{\rm PE}$ is proportional to the quantum efficiency (QE) of PMT, ϵ^2, and the number of photons that reach the end of the scintillator (N_γ). The ϵ^2 term comes from the fact that the energy loss of a charged particle in matter is proportional to Q^2. In order to calculate N_γ a `GEANT4` [25] simulation is performed. Using a $5\times5\times150$ cm^3 BC-408 scintillator with a surface reflectivity of 98%, N_γ is 8.3×10^5. Taking QE into account, $N_{\rm PE}$ is $2.5\times10^5\epsilon^2$. Once we have $N_{\rm PE}$ and P, the total number of signal events measured by the detector can be calculated as $s = N_\chi P$.

Figure 3 shows the 95% CL exclusion curve for $N_{\rm POT} = 10^{22}$. SUBMET provides the exclusion down to $\epsilon = 5\times10^{-5}$ in $m_\chi < 0.2$ GeV/c^2 and $\epsilon = 8\times10^{-4}$ in $m_\chi < 1.6$ GeV/c^2. Systematic uncertainty on b is not considered because it does not have a significant impact on the exclusion limit (table 1). The sudden degradation of sensitivity at $m_\chi = 0.2$GeV/c^2 is because of the small production rate of J/ψ with the 30 GeV proton beam.

The number of signal events recorded by the detector drops rapidly for $\epsilon < 10^{-3}$ due to small $N_{\rm PE}$. Therefore, increasing $N_{\rm PE}$ or N_χ does not have a large impact on the sensitivity in this phase space. This will be discussed in a quantitative way in the next section.

JHEP05(2021)031

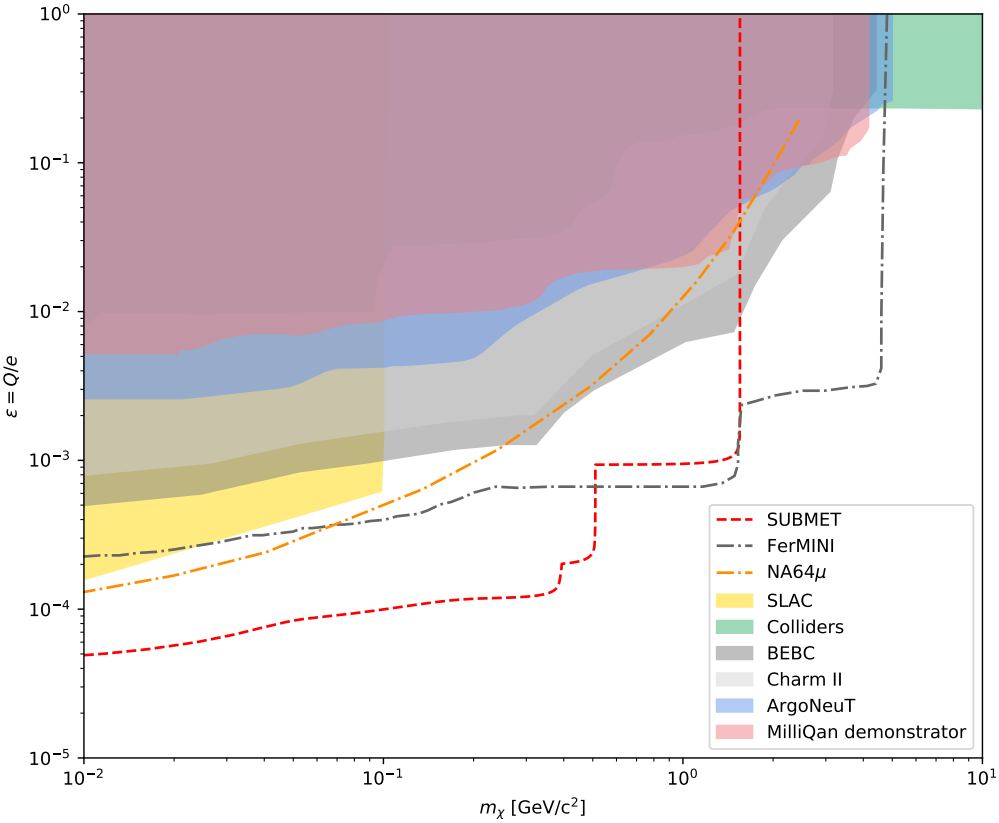

Figure 3. Exclusion at 95% CL for $N_{\mathrm{POT}} = 10^{22}$. The constraints from previous experiments are shown as shaded areas. The expected sensitivity of FerMINI [15] is drawn in the gray dotted line. There are other proposed experiments [22, 27], but only FerMINI with the NuMI beam and NA64μ [28] are included because they are in a similar time scale of SUBMET (within the next 5 years).

6 Alternative detector design

The sensitivity of the experiment depends on the configuration of the detector. This section describes the impact of a few key parameters for the detector design, focusing on the sub-millicharge regime. If further optimization of the detector is needed, this quantitative study can serve as a guide.

Searches in the sub-millicharge regime rely on the Poissonian fluctuation of small N_{PE}. Approximating $P \simeq N_{\mathrm{PE}}$ to the first order for small ϵ, we arrive at the following relation

$$s = N_{\epsilon=1,\chi}\epsilon^2(N_{\epsilon=1,\mathrm{PE}}\epsilon^2)^n \geq s^{95\%} \tag{6.1}$$

where s is the number of signal events, the subscript $\epsilon = 1$ means the values at $\epsilon = 1$ and $s^{95\%}$ is the number of signal events that provides 95% exclusion limit. Reordering in terms of ϵ, the exclusion limit at 95% CL is

$$\epsilon = \left(\frac{N^n_{\epsilon=1,\mathrm{PE}}N_{\epsilon=1,\chi}}{s^{95\%}}\right)^{-\frac{1}{2n+2}}. \tag{6.2}$$

JHEP05(2021)031

N_χ (relative)	$N_{\rm PE}$ (relative)	b (relative)	Exclusion limit on ϵ for $m_\chi = 10$ MeV/c^2
1	1	1	4.9×10^{-5}
2	1	1	4.6×10^{-5}
1/50	1	1	8.4×10^{-5}
1	1	25	6.0×10^{-5}
1	2	1	3.9×10^{-5}
1	0.8	1	5.3×10^{-5}

Table 1. Various detector configurations and their sensitivity. N_χ (relative) is the yields of signal events within the acceptance relative to the baseline, $N_{\rm PE}$ (relative) is the number of photon electrons relative to $N_{\rm PE} = 2.5 \times 10^5$, and b (relative) is the number of background events relative to $N_{\rm bkg} = 5$.

Due to the $\epsilon^{2(n+1)}$ term in (6.1), there is a sharp cutoff in s around $\epsilon \sim O(10^{-6})$. This limits the sensitivity to that regime, regardless of the detector configuration.

Table 1 shows different detector configurations and the corresponding exclusion limits for $m_\chi = 10$ MeV/c^2. The default configuration is in the first row; N_χ(relative)=1, $N_{\rm PE}$(relative)=1, and b(relative) = 1, where "relative" means relative to the values of the baseline configuration discussed in section 3.

The improvements achieved by extending the duration of data collection or making the detector area larger, e.g., adding more bars to each layer, are modest. Extending the duration or the detector area by a factor of 2 increases N_χ by the same amount. Sensitivity is improved by less than 10% (2$^{\rm nd}$ row in table 1). If the area of the detector is reduced to 10×10 cm (a factor of 50) or if the duration of the data-taking period is shortened by 1/50 (roughly 3 weeks), the exclusion limit moves to 8.4×10^{-5} (3$^{\rm rd}$ row in table 1). The impact of b is limited as well. If b is increased by a factor of 25, which corresponds to the DCR of 500 Hz, the limit is degraded by only 20% (4$^{\rm th}$ row in table 1).

The 5$^{\rm th}$ row in table 1 shows that the most effective component to enhance sensitivity is $N_{\rm PE}$. Increasing $N_{\rm PE}$ by a factor of 2 improves the sensitivity by 20%. This can be achieved by using a scintillator material with a higher light yield or by extending the length of the scintillator. However, improvement using longer scintillators is limited in length > 150 cm due to the effect of light attenuation. The 6$^{\rm th}$ row corresponds to the case of scintillator length of 75 cm. The degradation of sensitivity is only 10 %, which allows for a smaller-scale detector without a significant loss of performance.

Though $N_{\rm PE}$ plays the main role in enhancing sensitivity to sub-millicharged particles, the exclusion limit with the 0.5×0.5 m^2 detector is still in the range of $\epsilon = (3.9-6.0) \times 10^{-5}$ with the variations considered. This indicates that the sensitivity does not strongly depend on the configuration of the detector.

In the case of an unexpectedly large number of background events, installing additional layers can be considered to control them. Using 3 layers and assuming 0 background events, the exclusion limit reaches $\epsilon = 1.1 \times 10^{-4}$. The experiment still outperforms previous searches in this configuration.

JHEP05(2021)031

7 Discussion and conclusion

We propose a new experiment, SUBMET, sensitive to millicharged particles produced at the 30 GeV proton fixed-target collisions at J-PARC. The detector, inspired by the milliQan experiment, is based on long scintillators and is located in the Neutrino Monitor building 280 m from the target. With 10^{22} protons on target, the experiment is sensitive to particles with electric charge $5 \times 10^{-5}\, e$ for mass less than 0.2 GeV/c^2 and $8 \times 10^{-4}\, e$ for mass less than 1.6 GeV/c^2.

SUMBET would place the best limit in the low mass region $m_\chi < 0.2$ GeV/c^2 among existing and proposed experiments. In this regime, the N_{PE} is very small, so the probability of observing a photon produced by millicharged particles per layer ($P_{\text{layer}} = (1 - e^{-N_{\text{PE}}})$) is extremely small. Since the total probability is a power of P_{layer} by the number of layers, using two layers significantly enhances the probability compared to the detector designs with 3 or 4 layers. In the single-photoelectron regime, contributions from cosmic and radioactive backgrounds are expected to be suppressed because of the large number of photoelectrons they produce and the effective data-taking time (< 100 s for 3 years) due to correlation with the presence of the beam. In the end, they are sensitive to the environment the detector is in, so they need to be measured *in situ*.

Note that this experiment is complementary to the existing proposals [15, 22, 29] since the main interest is in the low mass region. The center of mass energy of the proton-target collisions is 7.5 GeV, and this limits the mass reach of the experiment to below $m_{J/\psi}/2$, while other proposals can cover higher mass regions. Compared to the FerMINI experiment, the production rate of J/ψ is much smaller due to lower beam energy. Therefore, the sensitivity to the χs from J/ψ decay is slightly worse, though it is still competitive.

We only consider the production of χs from the primary meson decays, but they can be produced from the electromagnetic component of the hadronic shower in the beam dump. The fact that its contribution is sensitive to both the geometry and the material of the surrounding environment makes the estimation complicated. Thus, we leave this study to future work.

A few detector designs to achieve an optimal sensitivity were considered in section 6, and we found that the configuration of the detector generally does not affect sensitivity. In addition, the operation of the upgraded proton beam at J-PARC will start in early 2022 [21]. These indicate that it is very important to install the detector as early as possible to fully exploit the upgraded power of the beam.

Acknowledgments

Authors would like to thank Tsutomu Mibe, Yoshiaki Fujii, Takeshi Nakadaira, and Toshifumi Tsukamoto for the insightful discussions on the detector site. In particular, we thank Toshifumi Tsukamoto for taking photographs of the Neutrino Monitor building so that we were able to understand the spatial constraints inside the building. We thank the members of the milliQan collaboration, particularly, Andy Hass, Christopher S. Hill, and David Stuart for the discussions at various stages of this study. We thank Matthew Citron, Albert

JHEP05(2021)031

De Roeck, Seung Joon Lee, and Eunil Won for providing comments on the draft. We thank Masashi Yokoyama for discussions regarding the schedule of the neutrino beamline. We also thank Hong Joo Kim for the information on the properties of various scintillation materials. This work has been supported by a Korea University Grant.

References

[1] N. Arkani-Hamed, D.P. Finkbeiner, T.R. Slatyer and N. Weiner, *A Theory of Dark Matter*, *Phys. Rev. D* **79** (2009) 015014 [arXiv:0810.0713] [INSPIRE].

[2] M. Pospelov and A. Ritz, *Astrophysical Signatures of Secluded Dark Matter*, *Phys. Lett. B* **671** (2009) 391 [arXiv:0810.1502] [INSPIRE].

[3] J.D. Bowman, A.E.E. Rogers, R.A. Monsalve, T.J. Mozdzen and N. Mahesh, *An absorption profile centred at 78 megahertz in the sky-averaged spectrum*, *Nature* **555** (2018) 67 [arXiv:1810.05912] [INSPIRE].

[4] R. Barkana, *Possible interaction between baryons and dark-matter particles revealed by the first stars*, *Nature* **555** (2018) 71 [arXiv:1803.06698] [INSPIRE].

[5] B. Holdom, *Two* U(1)*'s and* ϵ *Charge Shifts*, *Phys. Lett. B* **166** (1986) 196 [INSPIRE].

[6] E. Izaguirre and I. Yavin, *New window to millicharged particles at the LHC*, *Phys. Rev. D* **92** (2015) 035014 [arXiv:1506.04760] [INSPIRE].

[7] A.A. Prinz et al., *Search for millicharged particles at SLAC*, *Phys. Rev. Lett.* **81** (1998) 1175 [hep-ex/9804008] [INSPIRE].

[8] CMS collaboration, *Search for Fractionally Charged Particles in pp Collisions at* $\sqrt{s} = 7$ *TeV*, *Phys. Rev. D* **87** (2013) 092008 [arXiv:1210.2311] [INSPIRE].

[9] CMS collaboration, *Searches for Long-Lived Charged Particles in pp Collisions at* $\sqrt{s} = 7$ *and* 8 *TeV*, *JHEP* **07** (2013) 122 [arXiv:1305.0491] [INSPIRE].

[10] A. Ball et al., *Search for millicharged particles in proton-proton collisions at* $\sqrt{s} = 13$ *TeV*, *Phys. Rev. D* **102** (2020) 032002 [arXiv:2005.06518] [INSPIRE].

[11] G. Marocco and S. Sarkar, *Blast from the past: Constraints on the dark sector from the BEBC WA66 beam dump experiment*, *SciPost Phys.* **10** (2021) 043 [arXiv:2011.08153] [INSPIRE].

[12] S. Davidson, B. Campbell and D.C. Bailey, *Limits on particles of small electric charge*, *Phys. Rev. D* **43** (1991) 2314 [INSPIRE].

[13] ArgoNeuT collaboration, *Improved Limits on Millicharged Particles Using the ArgoNeuT Experiment at Fermilab*, *Phys. Rev. Lett.* **124** (2020) 131801 [arXiv:1911.07996] [INSPIRE].

[14] T. Emken, R. Essig, C. Kouvaris and M. Sholapurkar, *Direct Detection of Strongly Interacting Sub-GeV Dark Matter via Electron Recoils*, *JCAP* **09** (2019) 070 [arXiv:1905.06348] [INSPIRE].

[15] K.J. Kelly and Y.-D. Tsai, *Proton fixed-target scintillation experiment to search for millicharged dark matter*, *Phys. Rev. D* **100** (2019) 015043 [arXiv:1812.03998] [INSPIRE].

JHEP05(2021)031

[16] T. Sjöstrand et al., *An introduction to PYTHIA 8.2*, *Comput. Phys. Commun.* **191** (2015) 159 [arXiv:1410.3012] [INSPIRE].

[17] T2K collaboration, *Measurement of the muon beam direction and muon flux for the T2K neutrino experiment*, *PTEP* **2015** (2015) 053C01 [arXiv:1412.0194] [INSPIRE].

[18] HERA-B collaboration, *Measurement of the J/ψ production cross section in 920-GeV/c fixed-target proton-nucleus interactions*, *Phys. Lett. B* **638** (2006) 407 [hep-ex/0512029] [INSPIRE].

[19] T2K NEUTRINO BEAMLINE GROUP collaboration, *J-PARC Neutrino Beamline and 1.3 MW Upgrade*, *PoS* **NuFact2019** (2020) 054 [arXiv:2004.06877] [INSPIRE].

[20] T2K collaboration, *The T2K Experiment*, *Nucl. Instrum. Meth. A* **659** (2011) 106 [arXiv:1106.1238] [INSPIRE].

[21] M. Friend, *J-PARC accelerator and neutrino beamline upgrade programme*, *J. Phys. Conf. Ser.* **888** (2016) 012042.

[22] A. Ball et al., *A Letter of Intent to Install a milli-charged Particle Detector at LHC P5*, arXiv:1607.04669 [INSPIRE].

[23] D.E. Groom, N.V. Mokhov, S.I. Striganov, *Muon stopping power and range tables 10-MeV to 100-TeV*, *Atom. Data Nucl. Data Tabl.* **78** (2001) 183.

[24] K. Abe et al., *Measurements of the T2K neutrino beam properties using the INGRID on-axis near detector*, *Nucl. Instrum. Meth. A* **694** (2012) 211 [arXiv:1111.3119] [INSPIRE].

[25] GEANT4 collaboration, *GEANT4: a simulation toolkit*, *Nucl. Instrum. Meth. A* **506** (2003) 250 [INSPIRE].

[26] SAINT-GOBAIN *plastic scintillators*, accessed: 2020-08-17, https://www.crystals.saint-gobain.com/products/bc-408-bc-412-bc-416.

[27] R. Harnik, Z. Liu and O. Palamara, *Millicharged Particles in Liquid Argon Neutrino Experiments*, *JHEP* **07** (2019) 170 [arXiv:1902.03246] [INSPIRE].

[28] S.N. Gninenko, D.V. Kirpichnikov and N.V. Krasnikov, *Probing millicharged particles with NA64 experiment at CERN*, *Phys. Rev. D* **100** (2019) 035003 [arXiv:1810.06856] [INSPIRE].

[29] S. Foroughi-Abari, F. Kling and Y.-D. Tsai, *FORMOSA: Looking Forward to Millicharged Dark Sectors*, arXiv:2010.07941 [INSPIRE].

JHEP05(2021)031